ACS APPLIED NANO MATERIALS

www.acsanm.org Letter

Bromine Etching of Patterned $YBa_2Cu_3O_{6+x}$ Nanoscale Thin Films for High-Temperature Superconducting Devices

Miranda L. Vinay, Jay C. LeFebvre, Han Cai, Joseph Forman, and Shane Cybart*

Cite This: *ACS Appl. Nano Mater.* 2021, 4, 12926−12931 Read Online

ACCESS | Metrics & More | Article Recommendations | Supporting Information

ABSTRACT: Cuprate high-temperature superconducting (HTS) thin films like $YBa_2Cu_3O_{6+x}$ (YBCO) are subject to reduction reactions with CO_2 and H_2O. This poses a challenge for processing and storing nanoscale devices made from these films. A 1% bromine−ethanol etchant solution was investigated as a facile processing method for thin 50 nm films of patterned YBCO. Raman scattering, EDS, AFM, and HIM imaging show changes in the surface morphology and composition. RT measurements show electrical changes to a depth of ∼3 nm after bromination and a slight reduction in T_c (86.5 to 86.4 K). We conclude that bromination of YBCO has minimal electrical consequences.

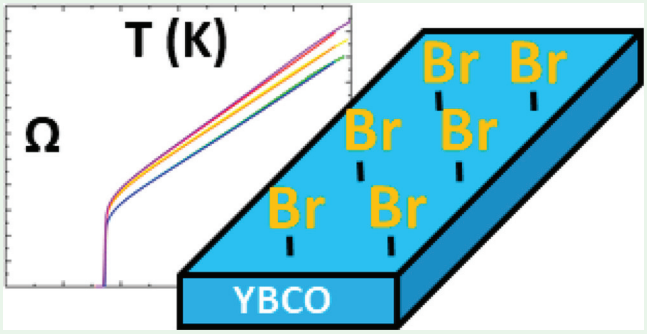

KEYWORDS: *YBCO, superconductor, bromine, etching, nanoscale devices*

High-temperature superconductivity was arguably one of the most exciting discoveries of the 20th century. The ceramic cuprate $YBa_2Cu_3O_{6+x}$ (YBCO) is one of the most popular high-temperature superconducting (HTS) materials, the thin films of which are used in variety of applications such as qubits in quantum computing,[1] analog to digital converters,[2] neuromorphic circuits,[3] and innumerable others. This HTS material boasts a critical temperature (T_c) of 93 K,[4] making superconducting devices more practical for consumer applications, as they can be cooled by liquid nitrogen (which has a boiling temperature of 77 K) instead of expensive liquid helium (which boils close to absolute zero at 4 K).

When used in devices such as Josephson junctions (JJs), the comprising superconducting thin films have thicknesses on the order of 20−200 nm.[5] New methods of JJ fabrication, such as Focused helium ion beam (FIB) technology, require even tighter thickness parameters, on the order of tens of nanometers, as the depth of beam penetration is dependent on the beam energy. The rate of environmental degradation is proportional to decreasing film thickness.[6] This creates urgency for new nanoscale-friendly processing for upcoming generations of fabricated devices, as thinner films are subject to faster rates environmental degradation because of an increased surface-area-to-volume-ratio.

The chemistry of YBCO degradation can be explained by reduction reactions with molecules in the air such as CO_2 and H_2O[7] depleting the saturation of oxygen within the crystal and leading to poorer electronic device performance, such as lowering T_c. In YBCO, electronic properties (and particularly the T_c) are variable and depend on the concentration of oxygen within the crystal lattice as it deviates from 6 to 7 mol per formula unit. Below a mole ratio of 6.2 O/f.u., superconductivity is completely destroyed as the material changes from a superconducting orthorhombic crystal structure to an insulating tetragonal unit cell.[8] Therefore, protecting YBCO and its precious high oxygen concentration presents challenges in the storage of YBCO-based devices such as JJs without compromising their superconducting performance.

From an electronic perspective, protecting this material from the environment poses a unique challenge for nanoscale devices. First, the superconducting state is facilitated by the mixed 2^+ and 3^+ oxidation states of copper atoms within the material. In turn, these oxidation states are linked to the concentration of oxygen. This is contradictory to most other passivation endeavors: YBCO must maintain oxidation, while traditional methods aim to prevent oxidation. Additionally, device processing methods must not interfere with their electrical performance, avoiding pitfalls such as lowering T_c or introducing $1/f$ noise into magnetic measurements from molecular surface adsorption

To this effort, previous methods of surface passivation for YBCO have been numerous and diverse, with several approaches purposefully damaging the surface of the film to

Received: September 24, 2021
Accepted: December 13, 2021
Published: December 14, 2021

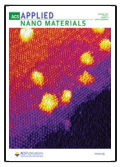

https://doi.org/10.1021/acsanm.1c03098
ACS Appl. Nano Mater. 2021, 4, 12926−12931

protect the remaining HTS film underneath.[9,10] Other methods use a variety of coatings, including metal,[11] oxide,[7] carbon,[12] and polymer coatings,[13] with some success for various applications. However, in order for this process to be optimized for nanoscale device fabrication, the method must avoid difficult processing, lattice mismatch (resulting in poor thermal cycling of the devices), the diffusion of metal ions into and out of the YBCO itself, and the diffusion of CO_2 and H_2O molecules through the coating. The majority of these studies have focused on bulk material or thick films (>100 nm), and are unexplored for nanoscale thin films. Furthermore, bromine is gaining popularity as both an etchant[14,15] and a passivation method for solar cells,[16,17] nanocrystals,[18] and silicon wafers.[19]

In this study, the chemical reagent bromine has been studied as a facile means of processing HTS cuprate surfaces without altering the electrical properties of the thin films. This study performed Br−surface reactions on 50 nm thick YBCO thin films. We expect the film to form several reaction products: copper(II) bromide, barium dibromide, and yttrium−bromide−oxygen complexes attached to the film's surface. This reaction can be found in eq 1.

$$Y_1Ba_2C_3O_{6+x} + 5.5Br_2 \xrightarrow{EtOH} 3CuBr_2 + 2BaBr_2 + YBrO_{x^-} \text{ and } CuBrO_{x^-} \quad (1)$$

Here, we investigate the effects of this product formation on the electrical properties of the 50 nm thin films as a foundation for future work with nanoscale electronics. Work by Lamine Mohamed Kollakoye Dieng proposed that bromine does not enter to YBCO lattice, but rather forms nanoclusters of lattice fragments of Br−O(4)−Ba−Cu(l)Cu(2) chains.[20] It is these surface interactions that are of interest to thin films and nanoelectronics, possibly serving as a means to maintain the oxygen content of the greater lattice in the film.

The films used in this study were patterned with a gold circuit via photolithography, the pattern of which and resulting device can found in Figure 1. The lingering products of the

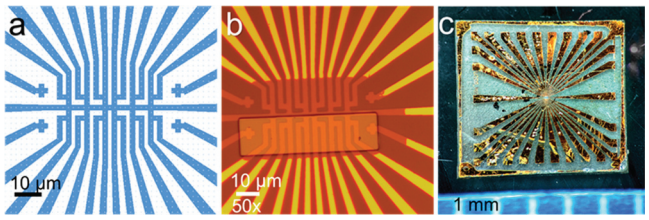

Figure 1. (a) Photolithography pattern, (b) patterned device circuitry, and (c) full chip after bromination, scale bar 1 mm.

reaction and the electrical consequences have been measured through Raman scattering, helium ion microscope (HIM) imaging, energy-dispersive X-ray spectroscopy (EDS), atomic force microscopy (AFM), and resistance−temperature (RT) measurements. This experiment allows us to precisely measure the electrical changes in the material after passivation in terms of electrical thickness, T_c, and residual resistivity.

Nanoscale images were taken of both surfaces via helium ion microscope (HIM) and atomic force microscopy (AFM). HIM images were taken of two patterned YBCO surfaces, one with bromine treatment and one without, and are shown in Figure 2. These images show the impact of bromine treatment on the YBCO surface. After treatment, the surface appears to be much more rough, with many inclusions when compared to the

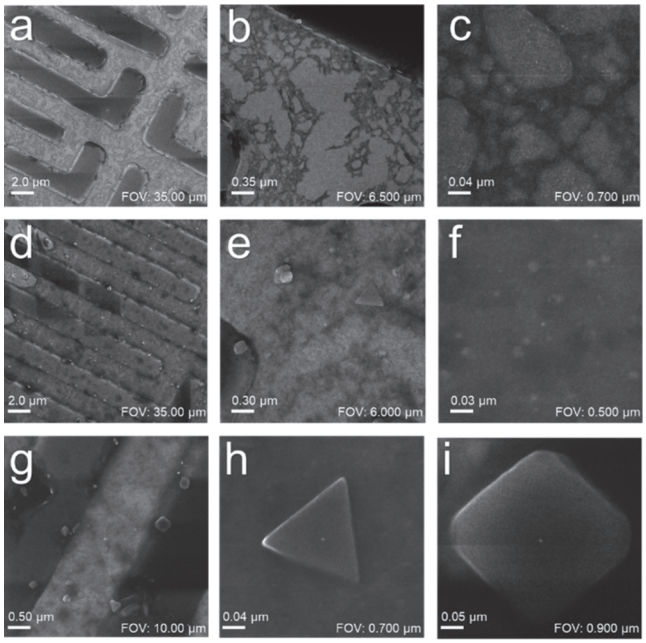

Figure 2. HIM images of the YBCO surface before (top) and after (middle) bromination at (a) 35.00, (b) 0.35, (c) 0.700, (d) 35.00, (e) 6.00, (f) 0.500 μm FOV. Images of crystalline shapes appearing on the surface of the brominated sample (bottom) with (g) many inclusions at 10.00 μm, (h) a triangular inclusion at 0.700 μm, and (i) a rhombic inclusion at 0.900 μm FOV.

untreated sample. Here, we observe several products on the order of hundreds of nanometers in scale that are stuck to the YBCO surface.

To further show the change in surface roughness, we took atomic force microscopy (AFM) images as shown in Figure 3. The top images show an identically fabricated patterned film and the bottom images show the film after bromine processing. From left to right, Figure 3a and c shows the samples via height sensing and Figure 3b and d shows the films via magnetic sensing. From these images, we can see a dramatic change in

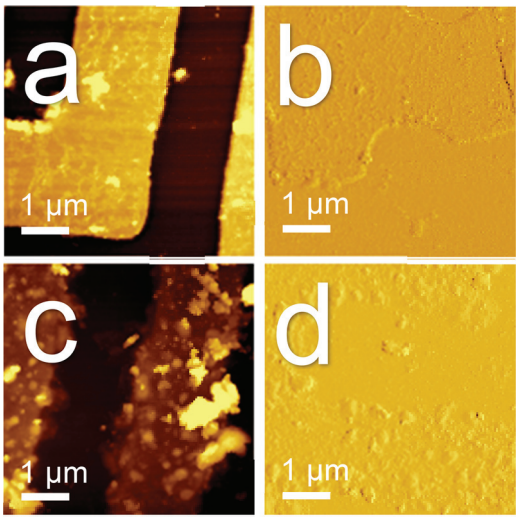

Figure 3. AFM images of (a, c) height profiles and (b, d) magnetic profiles of (a, b) unbrominated and (c, d) brominated patterned YBCO.

https://doi.org/10.1021/acsanm.1c03098
ACS Appl. Nano Mater. 2021, 4, 12926−12931

the surface morphology after the bromination process and an overall increase in surface roughness after treatment.

Compositional analysis to confirm the presence of bromine on the surface was done via Raman spectroscopy and energy-dispersive X-ray spectroscopy (EDS). The expected reaction products were taken from Vasquez et al. as well as Mukhopadhyay and Wei. Using photoelectron X-ray spectroscopy (XPS), they report products of YBr_3, $BaBr_3$, and CuBr in 1:4:3 product ratios[21] and YBr_3, $YBrO_3$ complexes, and electronic restructuring of Ba^{2+} and Cu^{2+} ions,[22] respectively. With these products in mind, Raman spectroscopy was performed on both unbrominated and brominated samples. Figure 4 shows a Raman spectra taken from 100 to 750 cm^{-1}

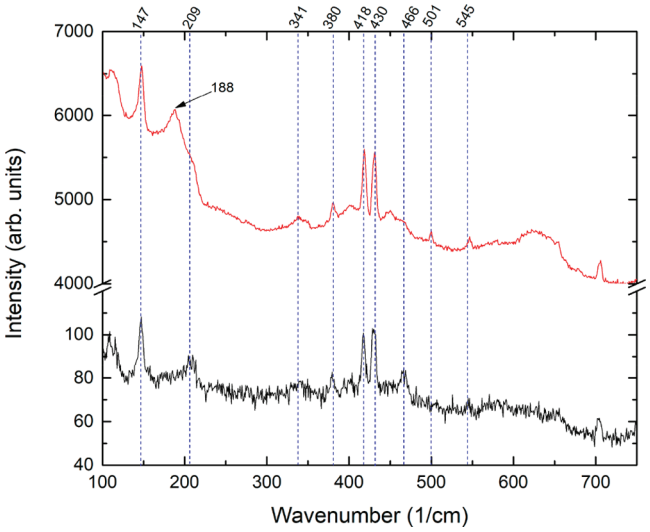

Figure 4. Raman spectra of YBCO on a sapphire substrate from 100 to 750 cm^{-1}. The black line represents an unbrominated sample and the red represents a brominated sample.

of characteristic YBCO peaks for the brominated (red) and unbrominated (black) samples. Comparing the two spectra, historically identifiable shared peaks are as follows: ~147 cm^{-1}, which has been reported to be a Cu-B_{2g} vibration,[23] likely within the YBCO structure and its environmental reduction reaction products but shifted by ~2 cm^{-1} from the original 1992 study. The peak at ~209 cm^{-1}, which has been reported to be a O(4) B_{2g} vibration inside of YBCO;[24] and ~340 cm^{-1} has been reported by several authors to be an O(2,3)-B_{1g} vibration.[25] Peaks at ~380, ~418, and ~430 cm^{-1} have been identified by Lorenz et al. to arise from the sapphire substrate supporting the YBCO thin film.[26] At ~466 cm^{-1}, an ~2 cm^{-1} shift occurs between the unbrominated (466 cm^{-1}) and brominated (467 cm^{-1}) samples. Both of these samples show a shift from the literature data, which present a peak characteristic of tetragonal-phase YBCO at ~463 cm^{-1}.[25] A theoretical peak reported by Thomsen et al. reports an O(2,3)-B_{3g} vibration at 544 cm^{-1}, which is seen in this spectra at ~545 cm^{-1} in the unbrominated spectrum and shift to ~547 cm^{-1} in the brominated sample.[27]

Peaks shown in both spectra at ~109, ~403, and ~704 cm^{-1} have not been identified and require further study. Peaks that were not seen in the unbrominated sample but that appear in the brominated sample include in this spectra peaks at ~188, ~501, and ~627 cm^{-1}. The first of these peaks may be evidence of reaction product remaining on the surface after the ethanol wash. Stepakova et. al reports a copper(II) bromide ($CuBr_2$) peak at ~189 cm^{-1}.[23] The second peak can be identified as an O(4)-A_g apex oxygen peak at ~500 cm^{-1}.[24] The collection of peaks centered around ~627 cm^{-1} take the same shape as those reported by Zhang et al. but are shifted from ~540 cm^{-1}. This could be due to the difference in film thickness.

Figure 5 shows unbrominated and brominated Raman spectra taken from 2300 to 2500 cm^{-1}. Although the Raman of

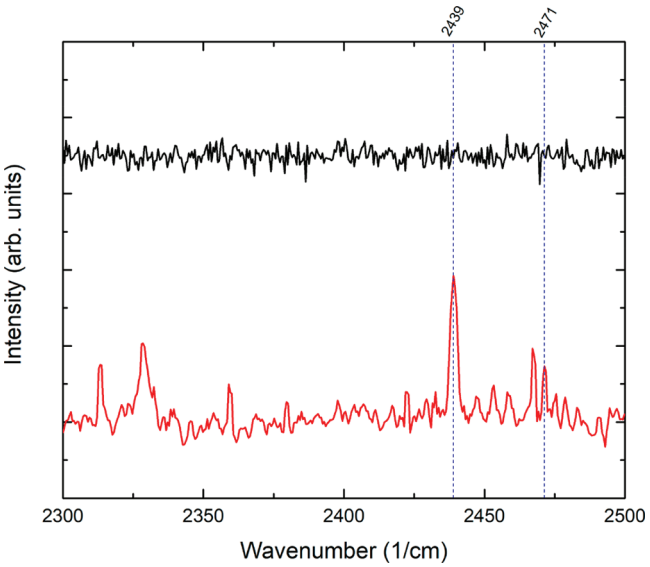

Figure 5. Raman spectra of unbrominated (black) and brominated (red) samples from 2300 to 2500 cm^{-1}. The sloped background was removed for the brominated sample.

the unbrominated sample shows minimal activity, two sets of Raman-active peaks are shown in the brominated sample at 2438 cm^{-1}. Apreyan et al. reports Raman-active peaks at ~2439 cm^{-1} to be bromic acid (HBr).[28]

After Raman analysis, further compositional analysis was done using energy-dispersive X-ray spectroscopy (EDS). This poses a particular challenge, as EDS software commonly misidentifies bromine and aluminum, because of their close characteristic energies, BrLα at 1.480 keV and AlKα at 1.487 keV, respectfully.[29] In our sample, the substrate contains aluminum, which will muddle the relative concentrations of each element. For this reason, only the higher-energy BrKα at 11.907 keV is reliable for element identification. The resulting spectra can be found in Figure 6, which depicts the higher-energy spectra with an inset showing a small, but present, bromine Kα peak. With this analysis, we can confirm the formation of bromine products on the surface.

Finally, to test the viability in application, we completed resistance−temperature (RT) measurements on the same sample before and after bromination that share similar electrical properties, as shown in Figure 7. Figure 5a shows a plot of resistance versus temperature for both the unbrominated YBCO and the brominated YBCO samples, as well as the same brominated YBCO sample measured 8 days after storage in air. As seen in the graph, there is good agreement between the cooling experiment and the following warming experiment. It should be noted that noise arising from contacts was eliminated in the warming experiment of the unbrominated sample. Additional characterization of the film arises

https://doi.org/10.1021/acsanm.1c03098
ACS Appl. Nano Mater. 2021, 4, 12926−12931

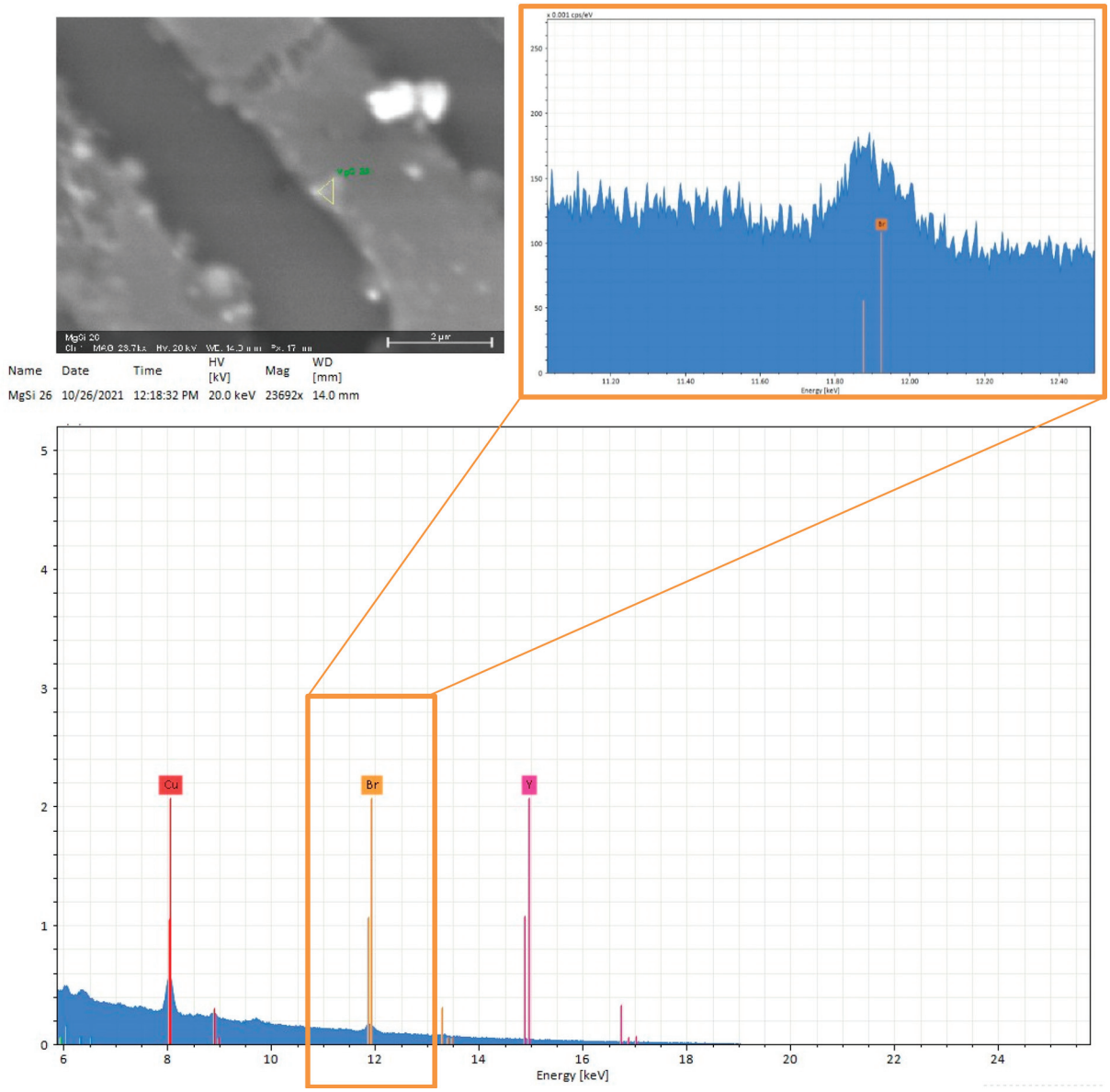

Figure 6. EDS spectra in the high-energy (6−24 keV) range. The inset shows the BrKα peak.

from the patterned YBCO surface, which allows for precise electrical measurements.

Additionally, as the bromine etches only the surface of the film, the electrical thickness of the brominated sample after the reaction can be found via mathematical calculation. The starting films were commercially purchased to be 50 nm thick, giving a resistivity calculation of 892.6 $\mu\Omega$/cm using the following calculation:

$$\rho_{290K} = \frac{Rtw}{L}$$

Where ρ is the resistivity in $\mu\Omega$/cm, R is the resistance at 290 K, t is the thickness of the film, w is the width of the channel, and L is the length of the channel. Using this relationship, we can calculate a new film thickness by assuming that the resistivity has not changed after treatment. Using the brominated film resistance at 290 K, the bromination reaction (1% Br in ethanol for 5 s) was found to poison the surface at 3 nm deep, leaving an effective electrical thickness of ∼47 nm.

Figure 7b shows the first derivative of the resistance from Figure 7a. From this manipulation, the T_c can be determined by the center of the peak. It can be seen that there are small differences in T_c between the unbrominated and brominated samples, with the brominated samples having a slightly lower critical temperature at 86.5 and 86.4 K, respectively. The brominated sample has a T_c of 86 K 1 week after bromination, indicating slight degradation of the thin film.

The literature reports several reaction products, namely, CuBr, $CuBr_2$, YBr_3, and $YBrO_3$ complexes. The AFM and HIM images show a distinct change in the YBCO surface before and after bromination, with several crystalline species forming on the surface. Although Vasquez et al. shows the possibility of both CuBr and $CuBr_2$ species forming after the bromination reaction, no evidence of CuBr peaks were found. However, there is the possibility of $CuBr_2$ formation, which has been characterized in this study by Raman spectroscopy with a forming in the brominated sample at ∼188 nm. Additionally, the rhombic structures appearing on the YBCO surface could be evidence of a monoclinic unit cell structure, which $CuBr_2$

https://doi.org/10.1021/acsanm.1c03098
ACS Appl. Nano Mater. 2021, 4, 12926−12931

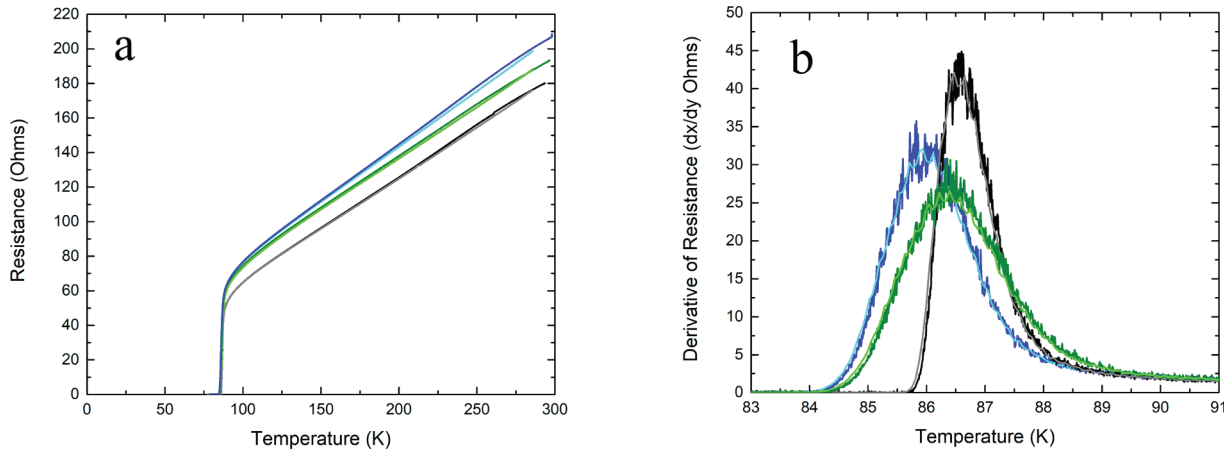

Figure 7. Electronic properties of a patterned YBCO sample before (black), immediately after the bromination reaction (green), and measured again 8 days after bromination (blue). (a) RT measurements, with slight variations in the starting resistances. (b) First derivative of the RT measurements in panel a. The darker lines represent the data taken from the cooling measurement ($T \rightarrow 77$ K), and the lighter colors represent that from the warming measurement.

has and CuBr does not (monoclinic versus cubic, respectively), but this speculation is qualitative. Combined, this data suggests that the bromine reacts with YBCO to form Cu^{2+} products, not Cu^{1+} products as postulated in the Vasquez et al. study. Further characterization such as compositional surface analysis is needed.

Additionally, although the Vasquez et al. and the Mukhopadhyay and Wei studies both showed evidence of the formation of YBr_3 after bromine etching, no Raman peaks could be identified against existing literature for this compound in this study. However, the $YBrO_3$ complexes postulated to be on the surface by XPS in previous studies have not yet been recorded via Raman spectroscopy and cannot be identified. As with the formation of the copper products, additional compositional surface analysis will be necessary to confirm surface species. Our results are consistent with the previous literature positing bromine as a nanocluster of copper and oxygen lattice fragments, but we are unable to exclude the existence of $YBrO_3$ compounds.

For electrical characterization, geometrically precise measurements were completed comparing unbrominated and brominated YBCO surfaces for the first time. Here, we found that lingering etchant products on the surface have a minimal impact on the performance of thin films. We conclude that these products should not impact the performance of thin films that are used in devices such as JJs and may serve as a possible means of facile processing that is easily integrated into device fabrication.

The summary of this study is as follows: Thin films of patterned YBCO were etched in dilute bromine-ethanol solution in an investigation for the deterioration of electronic performance with respect to nanoscale devices. Lingering reaction products on the surface are postulated to be $CuBr_2$ and possibly copper or yttrium bromine oxide complexes. Additionally, the bromination of the surface results in minor changes to the electrical properties of YBCO and leaves bromine processing as an avenue to explore for etching nanoscale films for HTS devices. Further work on this project may integrate this process into the fabrication of nanoscale electronic devices such as JJs and, ultimately, superconducting quantum interference devices (SQUIDS). It is necessary for further research to measure the impacts of such treatment on device performance.

■ ASSOCIATED CONTENT

Supporting Information

The Supporting Information is available free of charge at https://pubs.acs.org/doi/10.1021/acsanm.1c03098.

Additional experimental details, materials, and methods (PDF)

■ AUTHOR INFORMATION

Corresponding Author

Shane Cybart − *Department of Electrical and Computer Engineering, University of California Riverside, Riverside, California 92521, United States*; Email: cybart@ucr.edu

Authors

Miranda L. Vinay − *Department of Electrical and Computer Engineering, University of California Riverside, Riverside, California 92521, United States*; orcid.org/0000-0002-8883-7045

Jay C. LeFebvre − *Department of Electrical and Computer Engineering, University of California Riverside, Riverside, California 92521, United States*; orcid.org/0000-0001-8185-0602

Han Cai − *Department of Electrical and Computer Engineering, University of California Riverside, Riverside, California 92521, United States*

Joseph Forman − *Department of Electrical and Computer Engineering, University of California Riverside, Riverside, California 92521, United States*

Complete contact information is available at: https://pubs.acs.org/10.1021/acsanm.1c03098

Author Contributions

All authors have given approval to the final version of the manuscript.

Funding

This work is supported by NSF grant number 1664446 and AFOSR grant number FA9550-20-1-0144.

Notes

The authors declare no competing financial interest.

■ ACKNOWLEDGMENTS

We thank Robert Crowley III and Kevin Kou for the use of their fume hoods and chemicals and for the handling of hazardous chemicals. Additionally, we acknowledge the UC-Riverside Analytical Chemistry Instrumentation Facility for use of the Raman microscope and AFM instruments, as well as the Materials Science & Engineering Department and Eunsoo Lee for use of the SEM/EDS.

■ ABBREVIATIONS

HTS, high-temperature superconductor
YBCO, yttrium−barium−copper oxide
HIM, helium ion microscope
EDS, energy-dispersive X-ray spectroscopy
AFM, atomic force microscopy
RT, resistance−temperature
T_c, critical temperature
JJ, Josephson junction
FIB, focused ion beam
FOV, field of view

■ REFERENCES

(1) Amin, M. H. S.; Smirnov, A. Y.; Zagoskin, A. M.; Lindström, T.; Charlebois, S. A.; Claeson, T.; Tzalenchuk, A. Y. Silent Phase Qubit Based on D-Wave Josephson Junctions. *Phys. Rev. B: Condens. Matter Mater. Phys.* **2005**, *71* (6), 064516.
(2) McCambridge, J. D.; Forrester, M. G.; Miller, D. L.; Hunt, B. D.; Pryzbysz, J. X.; Talvacchio, J.; Young, R. M. Multilayer HTS SFQ Analog-to-Digital Converters. *IEEE Trans. Appl. Supercond.* **1997**, *7* (2), 3622−3625.
(3) Di Ventra, M.; Pershin, Y. V. Memory Materials: A Unifying Description. *Materials Today* **2011**, *14* (12), 584−591.
(4) Wu, M. K.; Ashburn, J. R.; Torng, C. J.; Hor, P. H.; Meng, R. L.; Gao, L.; Huang, Z. J.; Wang, Y. Q.; Chu, C. W. Superconductivity at 93 K in a New Mixed-Phase Yb-Ba-Cu-O Compound System at Ambient Pressure. *Phys. Rev. Lett.* **1987**, *58* (9), 908−910.
(5) Wu, C. H.; Jhan, F. J.; Chen, J. H.; Jeng, J. T.; Chen, K. L.; Yang, H. C. Fabrication and Properties of High- Tc YBCO Josephson Junction and SQUID with Variable Thickness Bridges by Focused Ion Beam. *IEEE Trans. Appl. Supercond.* **2011**, *21*, 375−378.
(6) Michaelis, A.; Irene, E. A.; Auciello, O.; Krauss, A. R. A Study of Oxygen Diffusion in and out of YBa2Cu3O7-δ Thin Films. *J. Appl. Phys.* **1998**, *83* (12), 7736−7743.
(7) Barkatt, A.; Hojaji, H.; Amarakoon, V. R.W.; Fagan, J. G. Environmental Stability of Higher Tc Superconducting Ceramics. *MRS Bull.* **1993**, *18* (9), 45−52.
(8) Friis Poulsen, H.; Hessel Andersen, N.; Vrtting Andersen, J.; Bohrt, H.; Mouritsen, O. G. Relation between Superconducting Transition Temperature and Oxygen Ordering in YBa2Cu3O6+x. *Nature* **1991**, *349* (6310), 594−596.
(9) Lam, S. K. H.; Bendavid, A.; Du, J. Trimming the Electrical Properties on Nanoscale YBa2Cu3O7−x Constrictions by Focus Ion Beam Technique. *Phys. C* **2017**, *540*, 38−43.
(10) Lee, D.; Condrate, R. A.; Taylor, J. A. Environmental Degradation Mechanism and Protective Organic Thin Film Coatings on a High-Temperature Bismuth-Cuprate Superconductor. *Phys. C* **2001**, *350* (1−2), 1−16.
(11) Shin, H.-S.; Kim, K.-H.; Dizon, J. R. C.; Kim, T.-Y.; Ko, R.-K.; Oh, S.-S. The Strain Effect on Critical Current in YBCO Coated Conductors with Different Stabilizing Layers. *Supercond. Sci. Technol.* **2005**, *18* (12), S364.
(12) Hentges, P. J.; Westwood, G.; Aubin, H.; Klemperer, W. G.; Greene, L. H. Solution-Growth of Ultra-Thin, Insulating Layers of Zirconia for Passivation and Tunnel Junction Fabrication on YBCO Thin Films. *IEEE Trans. Appl. Supercond.* **2003**, *13*, 801−804.
(13) Shan, Y. Q.; Fan, Z. G.; Du, J. H.; Gong, Q. L.; Cai, Y. M.; Wang, W. H.; Chen, L. L.; Zhao, Z. X. Steam Corrosion Dynamics and Protection for YBCO Superconductor. *Phys. C* **1997**, *282−287* (2), 497−498.
(14) Yue, C.; Sun, H.; Liu, W. J.; Guan, B.; Deng, X.; Zhang, X.; Yang, P. Environmentally Benign, Rapid, and Selective Extraction of Gold from Ores and Waste Electronic Materials. *Angew. Chem., Int. Ed.* **2017**, *56* (32), 9331−9335.
(15) Šik, O.; Bábor, P.; Polčák, J.; Belas, E.; Moravec, P.; Grmela, L.; Staněk, J. Low Energy Ion Scattering as a Depth Profiling Tool for Thin Layers - Case of Bromine Methanol Etched CdTe. *Vacuum* **2018**, *152*, 138−144.
(16) Yang, J.-N.; Song, Y.; Yao, J.-S.; Wang, K.-H.; Wang, J.-J.; Zhu, B.-S.; Yao, M.-M.; Rahman, S. U.; Lan, Y.-F.; Fan, F.-J.; Yao, H.-B. Potassium Bromide Surface Passivation on CsPbI3-XBrx Nanocrystals for Efficient and Stable Pure Red Perovskite Light-Emitting Diodes. *J. Am. Chem. Soc.* **2020**, *142* (6), 2956−2967.
(17) Parravicini, J.; Acciarri, M.; Lomuscio, A.; Murabito, M.; Le Donne, A.; Gasparotto, A.; Binetti, S. Gallium In-Depth Profile in Bromine- Etched Copper−Indium−Galium−(Di)Selenide (CIGS) Thin Films Inspected Using Raman Spectroscopy. *Appl. Spectrosc.* **2017**, *71* (6), 1334−1339.
(18) Jing, Q.; Zhang, M.; Huang, X.; Ren, X.; Wang, P.; Lu, Z. Surface Passivation of Mixed-Halide Perovskite CsPb(Br:XI1-x)3 Nanocrystals by Selective Etching for Improved Stability. *Nanoscale* **2017**, *9* (22), 7391−7396.
(19) Batra, N.; Vandana; Kumar, S.; Sharma, M.; Srivastava, S. K.; Sharma, P.; Singh, P. K. A Comparative Study of Silicon Surface Passivation Using Ethanolic Iodine and Bromine Solutions. *Sol. Energy Mater. Sol. Cells* **2012**, *100*, 43−47.
(20) Dieng, L. M. K. Understanding the Origin of the Recovery of Superconductivity in Halogenated YBCO Single Crystal Atomic Structure Study. *PhD Thesis*; Rutgers, The State University of New Jersey, Newark, NJ, 2004.
(21) Vasquez, R. P.; Foote, M. C.; Hunt, B. D. Reaction of Nonaqueous Halogen Solutions with YBa2Cu 3O7-X. *J. Appl. Phys.* **1989**, *66* (10), 4866−4877.
(22) Mukhopadhyay, S. M.; Wei, C. Interaction of Bromine with Y1Ba2Cu3O7-x: Its Role as a Dopant and an Etchant. *Phys. C* **1998**, *295* (3−4), 263−270.
(23) Stepakova, L. V.; Skripkin, M. Y.; Chernykh, L. V.; Starova, G. L.; Hajba, L.; Mink, J.; Sandström, M. Vibrational Spectroscopic and Force Field Studies of Copper(II) Chloride and Bromide Compounds, and Crystal Structure of KCuBr3. *J. Raman Spectrosc.* **2008**, *39* (1), 16−31.
(24) Thomsen, C.; Wegerer, R.; Habermeier, H. U.; Cardona, M. Determination of the Degree of Epitaxy in High-Tc Thin Films by Raman Spectroscopy. *Solid State Commun.* **1992**, *83* (3), 199−203.
(25) Barboy, I.; Camerlingo, C.; Bar, I.; Bareli, G.; Jung, G. Micro-Raman Spectroscopy of Laser Processed YBa 2Cu 3O 7-δ Thin Films. *J. Appl. Phys.* **2011**, *110* (3), 033912.
(26) Lorenz, M.; Hochmuth, H.; Natusch, D.; Börner, H.; Lippold, G.; Kreher, K.; Schmitz, W. Large-Area Double-Side Pulsed Laser Deposition of YBa 2 Cu 3 O 7−x Thin Films on 3-in. Sapphire Wafers ARTICLES YOU MAY BE INTERESTED IN. *Appl. Phys. Lett.* **1996**, *68*, 3332.
(27) Zhang, P.; Haage, T.; Habermeier, H. U.; Ruf, T.; Cardona, M. Raman Spectra of Ultrathin YBaCuO7-δ Films. *J. Appl. Phys.* **1996**, *80* (5), 2935−2938.
(28) Apreyan, R. A.; Karapetyan, H. A.; Petrosyan, A. M. Polymorphism of L-Nitroargininium Bromide Monohydrate. *J. Mol. Struct.* **2008**, *875* (1−3), 272−281.
(29) Newbury, D. E. Mistakes Encountered during Automatic Peak Identification in Low Beam Energy X-Ray Microanalysis. *Scanning* **2007**, *29* (4), 137−151.

https://doi.org/10.1021/acsanm.1c03098
ACS Appl. Nano Mater. 2021, 4, 12926−12931